Water Oxidation

International Edition: DOI: 10.1002/anie.201601799
German Edition: DOI: 10.1002/ange.201601799

Visible-Light-Driven Water Oxidation by a Molecular Manganese Vanadium Oxide Cluster

*Benjamin Schwarz+, Johannes Forster+, McKenna K. Goetz, Duygu Yücel, Claudia Berger, Timo Jacob, and Carsten Streb**

***Abstract:** Photosynthetic water oxidation in plants occurs at an inorganic calcium manganese oxo cluster, which is known as the oxygen evolving complex (OEC), in photosystem II. Herein, we report a synthetic OEC model based on a molecular manganese vanadium oxide cluster, $[Mn_4V_4O_{17}(OAc)_3]^{3-}$. The compound is based on a $[Mn_4O_4]^{6+}$ cubane core, which catalyzes the homogeneous, visible-light-driven oxidation of water to molecular oxygen and is stabilized by a tripodal $[V_4O_{13}]^{6-}$ polyoxovanadate and three acetate ligands. When combined with the photosensitizer $[Ru(bpy)_3]^{2+}$ and the oxidant persulfate, visible-light-driven water oxidation with turnover numbers of approximately 1150 and turnover frequencies of about 1.75 s^{-1} is observed. Electrochemical, mass-spectrometric, and spectroscopic studies provide insight into the cluster stability and reactivity. This compound could serve as a model for the molecular structure and reactivity of the OEC and for heterogeneous metal oxide water-oxidation catalysts.*

The sunlight-driven splitting of water into molecular oxygen and molecular hydrogen provides sustainable access to non-fossil-based fuels.[1,2] The four-electron oxidation of water to molecular oxygen is the more challenging half-reaction in water splitting. Water oxidation requires homogeneous[3–5] or heterogeneous[6–9] water oxidation catalysts (WOCs) that are both highly stable under oxidizing conditions and able to undergo multiple proton-coupled electron transfers.[3,10] In nature, light-driven water oxidation is accomplished by the oxygen evolving complex (OEC), the pentanuclear calcium manganese oxo cluster $[CaMn_4O_5]$ (Figure 1), located within a large protein assembly, namely photosystem II (PS II).[11,12] In vivo, the OEC is coordinatively stabilized by carboxylate- and imidazole-based amino acids.[13]

Since the first structural reports, the OEC has stimulated the development of synthetic molecular WOCs where metal oxo cores are stabilized by organic ligands.[14] Groundbreaking research focused on manganese oxo dimers,[15–18] whereas later studies used elaborately designed ligands to stabilize tetranuclear manganese oxo cubanes as functional OEC models.[19–22] Recently, ligand-stabilized calcium manganese oxo units such as $[CaMn_3O_4]^{6+}$[23] and $[CaMn_4O_4]^{9+}$[24] have been used to understand the influence of calcium on the OEC activity.

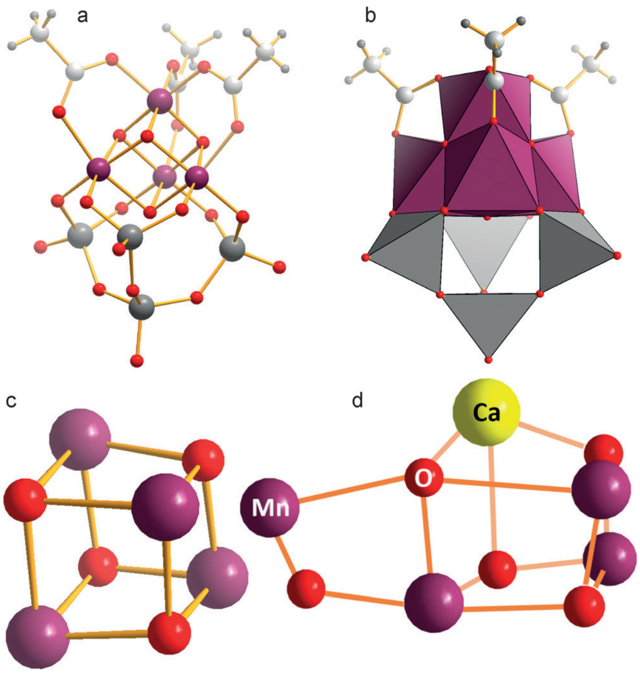

Figure 1. Structure of the manganese vanadium oxide $[Mn_4V_4O_{17}(OAc)_3]^{3-}$. a) Ball-and-stick and b) polyhedral representation. c) The $[Mn_4O_4]^{6+}$ cubane core. d) The calcium manganese oxo core of the OEC.[11] Mn purple, V gray, Ca yellow, O red, C gray, H small, gray.

The oxidative degradation of organic ligands under the harsh water-oxidation conditions is often perceived as a limitation of synthetic WOCs.[25] To address this challenge, molecular metal oxides that are stable towards oxidation, so-called polyoxometalates (POMs), have been introduced as highly robust ligands. POMs are early-transition-metal oxo clusters and typically based on vanadium, molybdenum, or tungsten in high oxidation states; their reactivity can be tuned by the incorporation of reactive metal centers.[26,27] Starting in 2008, Bonchio, Sartorel et al.,[28,29] and Hill et al.[30,31] reported the WOC activity of a ruthenium polyoxotungstate, $[Ru_4O_4(OH)_2(H_2O)_4(\gamma\text{-}SiW_{10}O_{36})_2]^{10-}$, under chemical[28,30] or photochemical conditions.[29,31]

---

[*] B. Schwarz,[+] Dr. J. Forster,[+] M. K. Goetz, Prof. Dr. C. Streb
Institute of Inorganic Chemistry I
Ulm University
Albert-Einstein-Allee 11, 89081 Ulm (Germany)
E-mail: carsten.streb@uni-ulm.de
Homepage: http://www.strebgroup.net
D. Yücel, C. Berger, Prof. Dr. T. Jacob
Institute of Electrochemistry
Ulm University
Albert-Einstein-Allee 47, 89081 Ulm (Germany)

[+] These authors contributed equally to this work.

Supporting information and the ORCID identification number(s) for the author(s) of this article can be found under http://dx.doi.org/10.1002/anie.201601799.

In 2010, Hill et al. reported the first non-precious-metal-based POM WOC, $[Co_4(H_2O)_2(\alpha\text{-}PW_9O_{34})_2]^{10-}$.[32,33] Under visible-light irradiation and in the presence of $[Ru(bpy)_3]^{2+}$ as a photosensitizer and $S_2O_8{}^{2-}$ as an oxidant, WOC activity with turnover numbers (TONs) up to 220 and turnover frequencies (TOFs) up to $0.25\,s^{-1}$ was observed.[32] Recently, Kortz, Bonchio, Scandola et al. reported the first manganese tungstate WOC, $[Mn_4O_3(OAc)_3(SiW_9O_{34})]^{6-}$, as a functional OEC model, where a defective manganese oxo cubane, $\{Mn^{III}{}_3Mn^{IV}O_3\}$, is stabilized by coordination to a lacunary silicotungstate anion and acetate ligands.[34]

Thus far, POM WOCs featuring polynuclear transition-metal oxo reaction sites have only been stabilized by tungstate ligands, and very little is known about the WOC activity of non-tungstate-based POM WOCs.[35,36] Building on our experience in metal-functionalized vanadates,[37–45] we investigated the incorporation of polynuclear manganese oxo units in vanadium oxide clusters and their use as OEC models.

Herein, we report the stabilization of an OEC-related, mixed-valent manganese oxo cubane in a manganese vanadium oxide cluster and its activity in visible-light-driven water oxidation. The title compound $(nBu_4N)_3[Mn_4V_4O_{17}(OAc)_3]\cdot 3\,H_2O$ ($=(nBu_4N)_3\mathbf{1}\cdot 3\,H_2O$) is formed from readily available precursors by one-pot self-assembly: The reaction of $(nBu_4N)_4[V_4O_{12}]$, $Mn(OAc)_3\cdot 2\,H_2O$, and $(nBu_4N)MnO_4$ in acetonitrile gives **1** as deep-brown single crystals in a yield of approximately 53%. The elemental composition was determined by elemental analysis, flame atomic absorption spectroscopy, and thermogravimetric analysis (see the Supporting Information). Single-crystal X-ray diffraction of **1** showed an anionic octanuclear cluster composed of a central $[Mn_4O_4]^{6+}$ cubane stabilized by a tripodal $[V_4O_{13}]^{6-}$ ligand and three acetate ligands (Figure 1). The $[Mn_4O_4]^{6+}$ unit is structurally related to the OEC, and similar Mn–O bond lengths were observed ($d_{Mn-O}(\mathbf{1}) \approx 1.8$–$2.1$ Å; $d_{Mn-O}(OEC) \approx 1.8$–$2.0$ Å).[11] The distance between adjacent manganese centers is $d_{Mn\cdots Mn} \approx 2.8$–$3.0$ Å (OEC: $d_{Mn\cdots Mn} \approx 2.8$–$3.3$ Å).[11]

The unique tripodal vanadate ligand $[V_4O_{13}]^{6-}$ interacts with three manganese centers of the cubane through six V–O–Mn coordination bonds. Notably, long-range attractive electrostatic interactions between one cubane oxo ligand and the four vanadium centers are observed, resulting in an elongation of the corresponding Mn–O bonds (ca. 2.1 Å) whereas the remaining Mn–O distances are significantly shorter (ca. 1.8–1.9 Å). The cubane geometry is therefore slightly distorted (see Figure 1c and the Supporting Information). The cubane coordination sphere is completed by three acetate ligands, leading to an idealized C_{3v} symmetry for **1** (Figure 1). Empirical bond valence sum (BVS) calculations based on crystallographic data gave a +5 oxidation state for all vanadium centers. For the manganese ions, an average oxidation state of approximately 3.6 was calculated, suggesting a mixed-valent $[Mn^{III}{}_2Mn^{IV}{}_2O_4]^{6+}$ cubane, which would correspond to the S_1 state of the OEC as assigned in the Kok cycle.[46]

Electrochemical and spectroscopic analyses support this assignment: Cyclic voltammetry of **1** in dry acetonitrile (containing 0.1 M $(nBu_4N)PF_6$ as the electrolyte) gave three quasi-reversible redox transitions centered at −1.0, 0.1, and 1.1 V (against Fc/Fc$^+$; see Figure 2a). Bulk electrolysis and linear sweep voltammetry of **1** showed that two consecutive one-electron oxidations are possible at $E = 0.65$ V and 1.35 V vs. Fc/Fc$^+$, respectively (see the Supporting Information), indicating that the S_2 ($Mn^{III}Mn^{IV}{}_3$) and S_3 ($Mn^{IV}{}_4$) states of the Kok cycle are accessible in **1**.[46] Electron paramagnetic resonance (EPR) spectroscopy (at $T = 11$ K, Figure 2b) was used to analyze **1** and the products of bulk electrolysis. Native **1** is EPR-silent and has a diamagnetic ground state; this is expected for mixed-valent $[Mn^{III}{}_2Mn^{IV}{}_2O_4]^{6+}$ cubanes and has been observed before.[47] In contrast, a complex EPR signal was observed for the one-electron-oxidized species; the signal is similar to those described in previous reports on related manganese oxo cubanes by Dismukes et al.[48] The two-electron-oxidized bulk-electrolysis species is EPR-silent (Figure 2b; see also the Supporting Information, for details).

ESI mass spectrometry of **1** in acetonitrile demonstrates the cluster stability in the solution/gas phase. Based on m/z and isotopic-pattern analysis, all three cluster-related signals feature mixed-valent manganese oxo cubanes: For example, at m/z 557.38 (calcd 557.38), the native species $(nBu_4N)[Mn^{III}{}_2Mn^{IV}{}_2V^{V}{}_4O_{17}(OAc)_3]^{2-}$ was observed (Figure 2b). In summary, all analyses point to a mixed-valent

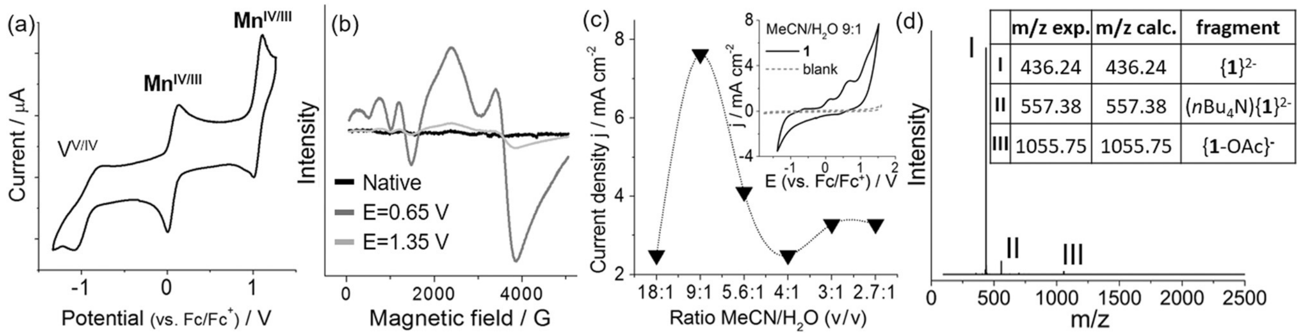

	m/z exp.	m/z calc.	fragment
I	436.24	436.24	$\{\mathbf{1}\}^{2-}$
II	557.38	557.38	$(nBu_4N)\{\mathbf{1}\}^{2-}$
III	1055.75	1055.75	$\{\mathbf{1}\text{-OAc}\}^{-}$

Figure 2. Reactivity of the manganese vanadate **1**. a) Cyclic voltammogram of **1** in dry MeCN (0.1 M $(nBu_4N)PF_6$, rest potential: −0.2 V). b) EPR spectrum ($T = 11$ K) of **1** and the one- and two-electron-oxidized species obtained by bulk electrolysis (in dry MeCN) at $E = 0.65$ V and 1.35 V (vs. Fc/Fc$^+$), respectively (see the Supporting Information). c) Electrochemical current density measurements of **1** (at 1.5 V vs. Fc/Fc$^+$) in mixed MeCN/H_2O solvents. Inset: Cyclic voltammogram of **1** in MeCN/H_2O (9:1, v/v). d) ESI mass spectrum of **1** in MeCN and table with the peak assignments; note that peaks I and III are one-electron-oxidized with respect to **1** (see also the Supporting Information).

$[Mn^{III}_2Mn^{IV}_2O_4]^{6+}$ cubane in ground-state **1**. The native cluster therefore represents a model compound of the S_1 state of the OEC, and our data suggest that electrochemical access to the S_2 and S_3 states of the Kok cycle is possible.

To identify optimal conditions for studying the WOC activity of **1**, cyclic voltammetry of **1** in acetonitrile/water mixtures of various compositions was performed. As shown in Figure 2c, the highest oxidative current densities (at $E=1.5$ V vs. Fc/Fc^+) were observed for an acetonitrile/water ratio of 9:1 (v/v), and the onset of the electrocatalytic water oxidation was observed at $E\approx0.95$ V vs. Fc/Fc^+ (see Figure 2c and the Supporting Information). The following WOC studies were therefore performed in this solvent mixture.

The visible-light-driven WOC activity of **1** was examined by combining **1** (0.3–10 μM) with the photosensitizer $[Ru(bpy)_3]^{2+}$ (1 mM) and the electron acceptor $S_2O_8^{2-}$ (10 mM) in deoxygenated acetonitrile/water (9:1, v/v). The system was irradiated with visible light (LED light source, $\lambda_{max}=470$ nm), and the oxygen evolution was continuously measured with a fiber-optic oxygen sensor in the reaction mixture (Figure 3).

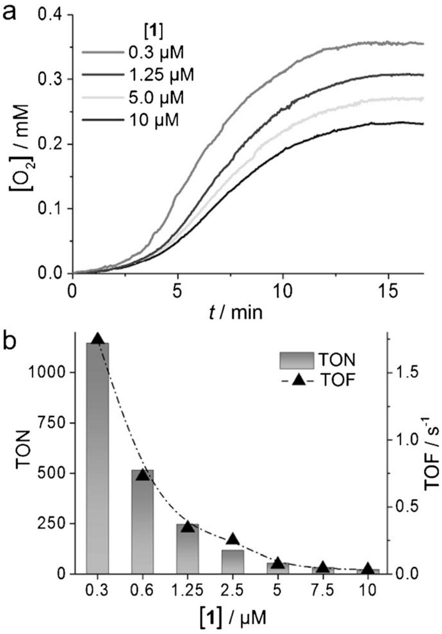

Figure 3. a) Visible-light-driven water oxidation with **1** (0.3–10 μM) in the presence of $[Ru(bpy)_3]^{2+}$ (1 mM) and $S_2O_8^{2-}$ (10 mM) in $MeCN/H_2O$ (9:1, v/v). b) TON and TOF of the visible-light-driven water oxidation with **1**. $TON=[O_2]_{final}/[\mathbf{1}]$, $TOF=[O_2]/([\mathbf{1}]\times t_{irradiation})$.

Oxygen evolution followed a sigmoidal trace, reaching a plateau after $t_{irradiation}\approx15$ min. An initial induction phase (ca. 3 min) was observed, which might be related to a catalyst activation step where the loss of acetate ligands is necessary to generate water-binding sites on the manganese oxo cubane. Similar behavior has been reported for a related phosphinate-stabilized manganese oxo catalyst.[20] Oxygen evolution is dependent on the catalyst concentration (Figure 3), and the maximum TONs (ca. 1150) and TOFs (ca. $1.75\ s^{-1}$) were observed at $[\mathbf{1}]=0.3$ μM (see the Supporting Information).

The reduced turnover numbers at increased catalyst concentrations could be related to the aggregation of the anionic catalyst with the cationic photosensitizer, resulting in colloid formation. At low concentrations of **1** (0.6 μM), no colloids were detected before and after irradiation by dynamic light scattering (DLS), microfiltration, and UV/Vis spectroscopy (see the Supporting Information),[49] highlighting that the reaction solution is homogeneous. In contrast, for high catalyst concentrations (10 μM), colloid formation by ion aggregation was detected, which is in line with previous reports.[33,49–51] As the colloidal particles are catalytically inactive, a significant decrease in WOC activity was observed (the TON decreased by ca. 95%). These results highlight the need for truly homogeneous conditions for high WOC activity in photosensitized polyoxometalate-based water-oxidation catalysis.[49,51] As the study was performed in non-buffered $MeCN/H_2O$ solution (owing to solubility issues with **1** in buffered solutions), the solution pH value drops upon water oxidation, eventually leading to a loss of catalytic activity. This is possibly associated with protonation of the manganese oxo core of **1** as indicated by pH-dependent UV/Vis spectroscopy, which has been previously observed for related manganese oxo species (see the Supporting Information).[52,53] Initial catalyst recovery/recycling experiments showed the principal possibility of catalyst recycling, and three consecutive standard WOC runs ($[\mathbf{1}]=0.6$ μM) with a sum total TON of about 780 were performed. However, after run 3, a significant loss of catalytic activity (a decrease in TOF of ca. 70%) was observed, indicating catalyst deactivation during catalysis (see the Supporting Information).

In summary, we have reported the first molecular manganese vanadium oxide water-oxidation catalyst, $[Mn_4V_4O_{17}(OAc)_3]^{3-}$. Under visible-light irradiation, the cluster shows high WOC activity (TON ≈ 1150, TOF $\approx1.75\ s^{-1}$). Furthermore, this compound could serve as a model system for the oxygen-evolving complex in photosystem II as it features a mixed-valent manganese oxo cubane, $[Mn^{III}_2Mn^{IV}_2O_4]^{6+}$, corresponding to the S_1 state of the Kok cycle. The higher oxidation states S_2 and S_3 are accessible by electrochemical oxidation. Future work will investigate the mechanistic aspects of electron transfer and oxygen evolution to assess whether this cluster can be used to gain insight into the electronic processes within the OEC during water oxidation.

Experimental Section

Synthesis of **1**: $(nBu_4N)_4[V_4O_{12}]\cdot4H_2O$ (401.4 mg, 0.279 mmol, 1 equiv), $Mn(OAc)_3\cdot2H_2O$ (299.3 mg, 1.12 mmol, 4 equiv), and $(nBu_4N)MnO_4$ (101.6 mg, 0.281 mmol, 1 equiv) were dissolved in MeCN (16 mL); then, aqueous $(nBu_4N)OH$ solution (200 μl, 20 wt.%) was added. The reaction mixture was stirred vigorously for 1 h at room temperature. Diffusion of diethyl ether into the reaction mixture gave dark brown cubic single crystals of **1** that were suitable for X-ray diffraction. Yield: 238 mg (0.149 mmol, 53.3% based on V). Elemental analysis calcd [%] for $Mn_4V_4O_{26}N_3C_{54}H_{123}$: C 39.21, H 7.50, N 2.54, Mn 13.29, V 12.74; found: C 39.14, H 7.38, N 2.48, Mn 13.65, V 13.12.

Crystallographic data and structure refinement for **1**: $C_{54}H_{123}Mn_4N_3O_{26}V_4$, $M_r=1654.08\ g\,mol^{-1}$; $T=150(2)$ K. Cubic, space group $Pa\bar{3}$, $a = 24.6787(10)$, $V = 15030.3(11)$ Å^3, $Z = 8$, $R1 = 0.0730$, $wR2 = 0.1975$. CCDC 898055 (**1**) contains the supplementary crystallographic data for this paper. These data are provided free of charge by The Cambridge Crystallographic Data Centre.

Light-driven water oxidation: A de-aerated MeCN/H_2O (9:1, v/v) solution (10 mL) containing $[Ru(bpy)_3]^{2+}$ (1.0 mM), $Na_2S_2O_8$ (10 mM), and **1** (0.3–10 μM) was prepared under light exclusion. The homogeneous solution was irradiated with monochromatic visible light (LED, $\lambda_{max} = 470$ nm) under magnetic stirring, and the oxygen evolution was followed using an oxygen-sensitive optical sensor.

Acknowledgements

C.S. gratefully thanks the Fonds der Chemischen Industrie for a Liebig Fellowship. The Deutsche Forschungsgemeinschaft (DFG, STR1164/4-1), the DFG graduate school "Chemical Photocatalysis" (GRK1626, Regensburg University), Ulm University, Friedrich-Alexander-University Erlangen-Nuremberg, the Fonds der Chemischen Industrie, and the DAAD RISE program are acknowledged for financial support. The EU COST actions CM1202 (PerspectH2O) and CM1203 (PoCheMoN) are acknowledged for enabling fruitful interdisciplinary discussions. Experimental support by Oliver Tröppner (Prof. Dr. Ivana Ivanovic-Burmazovic; ESI-MS), Susanne Sihler (Prof. Dr. Tanja Weil; DLS), and Dr. Jörg Sutter (Prof. Dr. Karsten Meyer; EPR) is gratefully acknowledged.

Keywords: manganese · polyoxometalates · polyoxovanadates · self-assembly · water oxidation

How to cite: *Angew. Chem. Int. Ed.* **2016**, *55*, 6329–6333
Angew. Chem. **2016**, *128*, 6437–6441

---

[1] N. S. Lewis, D. G. Nocera, *Proc. Natl. Acad. Sci. USA* **2006**, *103*, 15729–15735.
[2] T. Faunce, S. Styring, M. R. Wasielewski, G. W. Brudvig, A. W. Rutherford, J. Messinger, A. F. Lee, C. L. Hill, H. deGroot, M. Fontecave, D. R. MacFarlane, B. Hankamer, D. G. Nocera, D. M. Tiede, H. Dau, W. Hillier, L. Wang, R. Amal, *Energy Environ. Sci.* **2013**, *6*, 1074–1076.
[3] H. Dau, C. Limberg, T. Reier, M. Risch, S. Roggan, P. Strasser, *ChemCatChem* **2010**, *2*, 724–761.
[4] B. Limburg, E. Bouwman, S. Bonnet, *Coord. Chem. Rev.* **2012**, *256*, 1451–1467.
[5] *Molecular Water Oxidation Catalysis* (Ed.: A. Llobet), Wiley, New York, **2014**.
[6] T. Hisatomi, J. Kubota, K. Domen, *Chem. Soc. Rev.* **2014**, *43*, 7520–7535.
[7] M. Woodhouse, B. A. Parkinson, *Chem. Soc. Rev.* **2009**, *38*, 197–210.
[8] J. R. Swierk, T. E. Mallouk, *Chem. Soc. Rev.* **2013**, *42*, 2357–2387.
[9] M. M. Najafpour, T. Ehrenberg, M. Wiechen, P. Kurz, *Angew. Chem. Int. Ed.* **2010**, *49*, 2233–2237; *Angew. Chem.* **2010**, *122*, 2281–2285.
[10] W. Lubitz, E. J. Reijerse, J. Messinger, *Energy Environ. Sci.* **2008**, *1*, 15–31.
[11] Y. Umena, K. Kawakami, J.-R. R. Shen, N. Kamiya, *Nature* **2011**, *473*, 55–60.
[12] N. Cox, D. A. Pantazis, F. Neese, W. Lubitz, *Acc. Chem. Res.* **2013**, *46*, 1588–1596.
[13] J. P. McEvoy, G. W. Brudvig, *Chem. Rev.* **2006**, *106*, 4455–4483.
[14] X. Liu, F. Wang, *Coord. Chem. Rev.* **2012**, *256*, 1115–1136.
[15] J. Limburg, J. S. Vrettos, L. M. Liable-Sands, A. L. Rheingold, R. H. Crabtree, G. W. Brudvig, *Science* **1999**, *283*, 1524–1527.
[16] R. Manchanda, G. W. Brudvig, R. H. Crabtree, *Coord. Chem. Rev.* **1995**, *144*, 1–38.
[17] C. W. Cady, R. H. Crabtree, G. W. Brudvig, *Coord. Chem. Rev.* **2008**, *252*, 444–455.
[18] M. L. A. Abrahamsson, H. Berglund Baudin, A. Tran, C. Philouze, K. E. Berg, M. K. Raymond-Johansson, L. Sun, B. Åkermark, S. Styring, L. Hammarström, *Inorg. Chem.* **2002**, *41*, 1534–1544.
[19] W. Rüttinger, G. C. Dismukes, *Chem. Rev.* **1997**, *97*, 1–24.
[20] G. C. Dismukes, R. Brimblecombe, G. A. N. Felton, R. S. Pryadun, J. E. Sheats, L. Spiccia, G. F. Swiegers, *Acc. Chem. Res.* **2009**, *42*, 1935–1943.
[21] R. Brimblecombe, G. F. Swiegers, G. C. Dismukes, L. Spiccia, *Angew. Chem. Int. Ed.* **2008**, *47*, 7335–7338; *Angew. Chem.* **2008**, *120*, 7445–7448.
[22] R. Brimblecombe, A. Koo, G. C. Dismukes, G. F. Swiegers, L. Spiccia, *J. Am. Chem. Soc.* **2010**, *132*, 2892–2894.
[23] J. S. Kanady, E. Y. Tsui, M. W. Day, T. Agapie, *Science* **2011**, *333*, 733–736.
[24] C. Zhang, C. Chen, H. Dong, J.-R. Shen, H. Dau, J. Zhao, *Science* **2015**, *348*, 690–693.
[25] H. Lv, Y. V. Geletii, C. Zhao, J. W. Vickers, G. Zhu, Z. Luo, J. Song, T. Lian, D. G. Musaev, C. L. Hill, *Chem. Soc. Rev.* **2012**, *41*, 7572–7589.
[26] *Special POM themed issue* (Eds.: L. Cronin, A. Müller), *Chem. Soc. Rev.* **2012**, *41*, 7325–7648.
[27] *Special POM issue* (Ed.: C. L. Hill), *Chem. Rev.* **1998**, *98*, 1–300.
[28] A. Sartorel, M. Carraro, G. Scorrano, R. De Zorzi, S. Geremia, N. D. McDaniel, S. Bernhard, M. Bonchio, *J. Am. Chem. Soc.* **2008**, *130*, 5006–5007.
[29] A. Sartorel, P. Miró, E. Salvadori, S. Romain, M. Carraro, G. Scorrano, M. Di Valentin, A. Llobet, C. Bo, M. Bonchio, *J. Am. Chem. Soc.* **2009**, *131*, 16051–16053.
[30] Y. V. Geletii, B. Botar, P. Kögerler, D. A. Hillesheim, D. G. Musaev, C. L. Hill, *Angew. Chem. Int. Ed.* **2008**, *47*, 3896–3899; *Angew. Chem.* **2008**, *120*, 3960–3963.
[31] Y. V. Geletii, Z. Huang, Y. Hou, D. G. Musaev, T. Lian, C. L. Hill, *J. Am. Chem. Soc.* **2009**, *131*, 7522–7523.
[32] Z. Huang, Z. Luo, Y. V. Geletii, J. W. Vickers, Q. Yin, D. Wu, Y. Hou, Y. Ding, J. Song, D. G. Musaev et al., *J. Am. Chem. Soc.* **2011**, *133*, 2068–2071.
[33] Q. Yin, J. M. Tan, C. Besson, Y. V. Geletii, D. G. Musaev, A. E. Kuznetsov, Z. Luo, K. I. Hardcastle, C. L. Hill, *Science* **2010**, *328*, 342–345.
[34] R. Al-Oweini, A. Sartorel, B. S. Bassil, M. Natali, S. Berardi, F. Scandola, U. Kortz, M. Bonchio, *Angew. Chem. Int. Ed.* **2014**, *53*, 11182–11185; *Angew. Chem.* **2014**, *126*, 11364–11367.
[35] S. Tanaka, M. Annaka, K. Sakai, *Chem. Commun.* **2012**, *48*, 1653–1655.
[36] M. V. Pavliuk, V. G. Makhankova, V. N. Kokozay, I. V. Omelchenko, J. Jezierska, A. Thapper, S. Styring, *Polyhedron* **2015**, *88*, 81–89.
[37] K. Kastner, J. T. Margraf, T. Clark, C. Streb, *Chem. Eur. J.* **2014**, *20*, 12269–12273.
[38] K. Kastner, J. Forster, H. Ida, G. N. Newton, H. Oshio, C. Streb, *Chem. Eur. J.* **2015**, *21*, 7686–7689.
[39] J. Forster, B. Rösner, R. H. Fink, L. C. Nye, I. Ivanovic-Burmazovic, K. Kastner, J. Tucher, C. Streb, *Chem. Sci.* **2013**, *4*, 418–424.
[40] A. Seliverstov, C. Streb, *Chem. Eur. J.* **2014**, *20*, 9733–9738.
[41] A. Seliverstov, J. Forster, M. Heiland, J. Unfried, C. Streb, *Chem. Commun.* **2014**, *50*, 7840–7843.
[42] A. Seliverstov, C. Streb, *Chem. Commun.* **2014**, *50*, 1827–1829.

[43] K. Kastner, B. Puscher, C. Streb, *Chem. Commun.* **2013**, *49*, 140–142.
[44] J. Tucher, L. C. Nye, I. Ivanovic-Burmazovic, A. Notarnicola, C. Streb, *Chem. Eur. J.* **2012**, *18*, 10949–10953.
[45] J. Tucher, K. Peuntinger, J. T. Margraf, T. Clark, D. M. Guldi, C. Streb, *Chem. Eur. J.* **2015**, *21*, 8716–8719.
[46] B. Kok, B. Forbush, M. McGloin, *Photochem. Photobiol.* **1970**, *11*, 457–475.
[47] W. F. Ruettinger, G. C. Dismukes, *Inorg. Chem.* **2000**, *39*, 1021–1027.
[48] W. F. Ruettinger, D. M. Ho, G. C. Dismukes, *Inorg. Chem.* **1999**, *38*, 1036–1037.
[49] B. Kirchhoff, S. Rau, C. Streb, *Eur. J. Inorg. Chem.* **2016**, *9*, 1425–1429.
[50] V. Artero, M. Fontecave, *Chem. Soc. Rev.* **2013**, *42*, 2338–2356.
[51] J. J. Stracke, R. G. Finke, *ACS Catal.* **2014**, *4*, 909–933.
[52] W. Ruettinger, M. Yagi, K. Wolf, S. Bernasek, G. C. Dismukes, *J. Am. Chem. Soc.* **2000**, *122*, 10353–10357.
[53] S. R. Cooper, M. Calvin, *J. Am. Chem. Soc.* **1977**, *99*, 6623–6630.

Received: February 20, 2016